Point mutations that inactivate MGAT4D-L, an inhibitor of MGAT1 and complex *N*-glycan synthesis

Received for publication, June 11, 2020, and in revised form, July 31, 2020 Published, Papers in Press, August 6, 2020, DOI 10.1074/jbc.RA120.014784

Ayodele Akintayo, Joshua Mayoral, Masahiro Asada, Jian Tang, Subha Sundaram, and Pamela Stanley*

From the Department of Cell Biology, Albert Einstein College of Medicine, New York, New York, USA

Edited by Gerald W. Hart

The membrane-bound, long form of MGAT4D, termed MGAT4D-L, inhibits MGAT1 activity in transfected cells and reduces the generation of complex *N*-glycans. MGAT1 is the GlcNAc-transferase that initiates complex and hybrid *N*-glycan synthesis. We show here that *Drosophila* MGAT1 was also inhibited by MGAT4D-L in S2 cells. In mammalian cells, expression of MGAT4D-L causes the substrate of MGAT1 ($Man_5GlcNAc_2Asn$) to accumulate on glycoproteins, a change that is detected by the lectin *Galanthus nivalis* agglutinin (GNA). Using GNA binding as an assay for the inhibition of MGAT1 in MGAT4D-L transfectants, we performed site-directed mutagenesis to determine requirements for MGAT1 inhibition. Deletion of 25 amino acids (aa) from the C terminus inactivated MGAT4D-L, but deletion of 20 aa did not. Conversion of the five key amino acids (PSLFQ) to Ala, or deletion of PSLFQ in the context of full-length MGAT4D-L, also inactivated MGAT1 inhibitory activity. Nevertheless, mutant, inactive MGAT4D-L interacted with MGAT1 in co-immunoprecipitation experiments. The PSLFQ sequence also occurs in MGAT4A and MGAT4B GlcNAc-transferases. However, neither inhibited MGAT1 in transfected CHO cells. MGAT4D-L inhibitory activity could be partially transferred by attaching PSLFQ or the 25-aa C terminus of MGAT4D-L to the C terminus of MGAT1. Mutation of each amino acid in PSLFQ to Ala identified both Leu and Phe as independently essential for MGAT4D-L activity. Thus, replacement of either Leu-395 or Phe-396 with Ala led to inactivation of MGAT4D-L inhibitory activity. These findings provide new insights into the mechanism of inhibition of MGAT1 by MGAT4D-L, and for the development of small molecule inhibitors of MGAT1.

Understanding factors that regulate glycosylation is critical for basic research into the functions of glycans in biology, and for practical reasons of glycosylation engineering for numerous purposes. Endogenous factors that regulate glycosyltransferase activity are few. For example, COSMC is a chaperone of the core 1 β1,3GalT C1GALT1, often termed T-synthase (reviewed in Ref. 1); Windbeutel is a chaperone of Pipe, a proteoglycan sulfotransferase in *Drosophila* (2); multi-transmembrane BAX inhibitor motif-containing proteins target Gb3 synthase to the lysosome and reduce the generation of glycolipid Gb3 (3); and ppGalNAcTs that initiate mucin glycan synthesis are stimulated by Src tyrosine kinase to relocate to the endoplasmic reticulum where they modify novel substrates (4). MGAT4D-L is a type II glycoprotein that binds to and inhibits the glycosyltransferse MGAT1 (5, 6). MGAT1 is a GlcNAc-transferase that transfers GlcNAc to $Man_5GlcNAc_2Asn$ on glycoproteins, and thereby initiates subsequent reactions that generate glycoproteins carrying hybrid and complex *N*-glycans (7).

MGAT4D was originally termed GlcNAc-T1 inhibitory protein (GnT1IP) (5), then GL54D (8), or MGAT4D by the Human Genome Nomenclature Committee, based on its sequence similarity to MGAT4 family members. When a cDNA encoding the N terminally extended, long form of MGAT4D (MGAT4D-L) is transfected into Chinese hamster ovary (CHO), or other mammalian cells, MGAT1 activity is specifically reduced in cell lysates (5). Transfected cells sorted for high expression of MGAT4D-L do not synthesize complex *N*-glycans (5). Consequently, MGAT4D-L transfectants are resistant to cytotoxic plant lectins that bind to complex *N*-glycans, and exhibit increased binding of lectins that recognize oligomannosyl *N*-glycans, which accumulate in the absence of MGAT1 (5). Thus, the Man-binding lectin GNA (*Galanthus nivalis* agglutinin) binds much better to CHO cells overexpressing MGAT4D-L than to CHO cells (5). MGAT4D-L forms heteromers with MGAT1 in the Golgi, but does not interact with other GlcNAc-transferases of the medial Golgi (6). Genome databases contain numerous open reading frames that encode type II transmembrane proteins with no known activity. Thus, MGAT4D-L may be the first in a new class of glycosylation regulator.

In this paper, we develop a flow cytometry assay for MGAT4D-L inhibitory activity, and determine MGAT4D-L amino acids (aa) required for inhibition of MGAT1. We identified five aa near the C terminus of MGAT4D-L that were essential for its inhibitory activity. Transfer of peptides containing these amino acids to the C terminus of MGAT1 conferred partial inhibition of MGAT1 activity. Further mutagenesis revealed two amino acids that were individually required for MGAT4D-L to inhibit MGAT1, Leu-395 or Phe-396.

Results

A flow cytometry assay of MGAT1 inhibition by MGAT4D-L

MGAT4D-L inhibits MGAT1 when it is overexpressed in transfected cells (5, 6). However, expression sufficient to inhibit

This article contains supporting information.

* For correspondence: Pamela Stanley, pamela.stanley@einsteinmed.org.

Present address for Joshua Mayoral: Dept. of Pathology, Albert Einstein College of Medicine, New York, New York, USA.

Present address for Masahiro Asada: Cellular and Molecular Biotechnology Research Institute, National Institute of Advanced Industrial Science and Technology (AIST), Tsukuba Central 5, 1-1-1 Higashi, Tsukuba, Ibaraki, Japan.

Present address for: Jian Tang: Elstar Therapeutics, Cambridge, Massachusetts, USA.

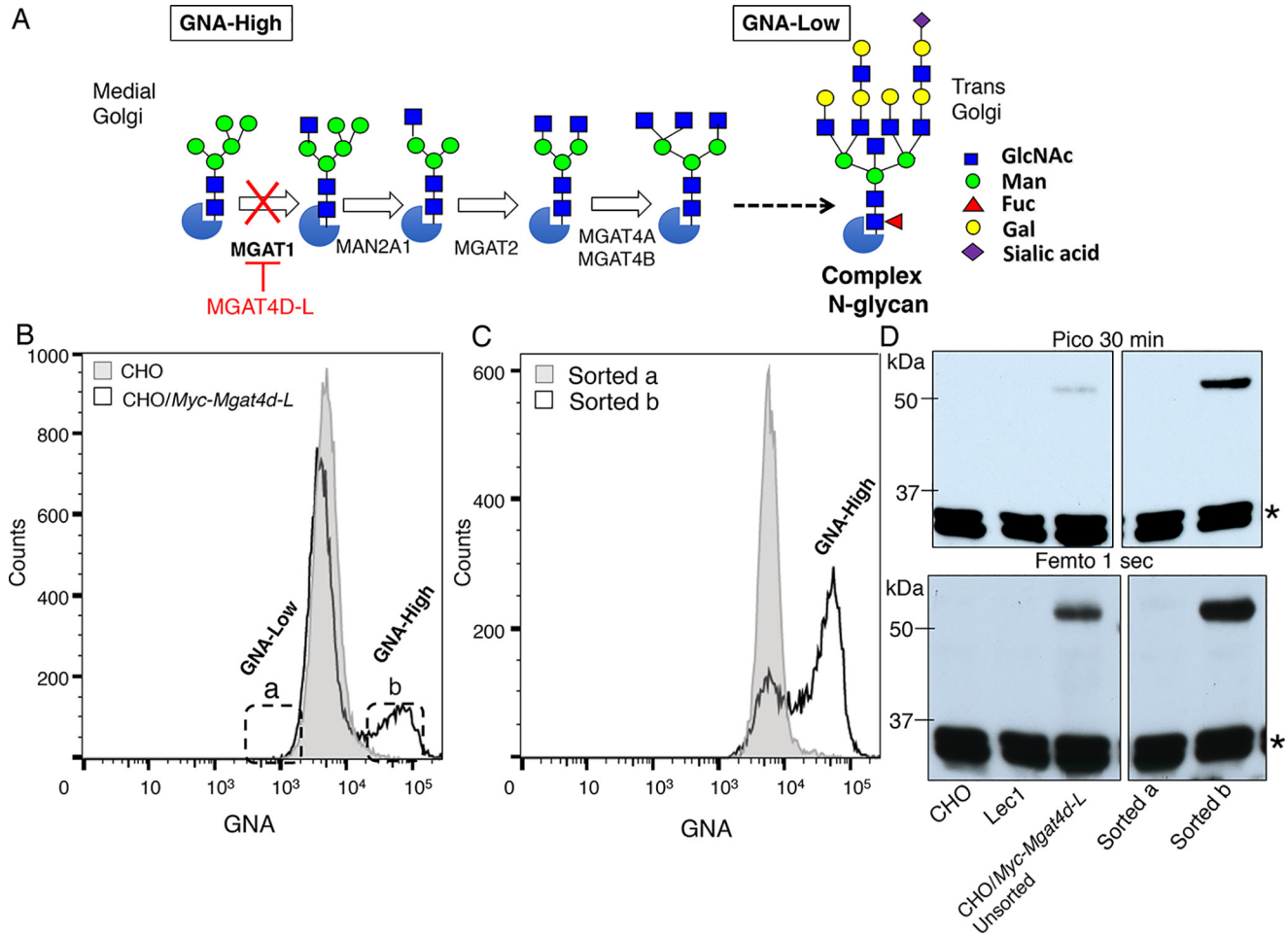

Figure 1. GNA-binding assay for inhibition of MGAT1 by MYC-MGAT4D-L. *A,* schematic representation of *N*-glycan maturation in the Golgi compartment showing the reaction catalyzed by MGAT1 and inhibited by MGAT4D-L. Sugar symbols conform to recommendations of the Symbol Nomenclature for Glycans (9, 10). *B,* GNA flow cytometry profile of CHO cells and CHO cells transfected with a *Myc-Mgat4d-L* cDNA. GNA-Low (*a*) and GNA-High (*b*) populations were sorted and briefly cultured, before being analyzed for GNA binding. *C,* GNA flow cytometry profiles of sorted populations from *panel B*. *D,* Western blots of proteins (50 μg/well) extracted from untransfected CHO or Lec1 CHO cells, *Myc-Mgat4d-L*-transfected CHO cells unsorted, GNA-Low (*sorted a*) and GNA-High (*sorted b*) populations. MYC-MGAT4D-L was detected using antibodies against MGAT4D-L N-terminal peptide. The blot was first treated with Pico PLUS chemiluminescent reagent and exposed to film for 30 min, then treated with Femto chemiluminescent reagent and exposed to film for 1 s. The enrichment of MYC-MGAT4D-L protein after sorting is most obvious from the Pico 30 min blot. * identifies nonspecific bands that served as loading control.

complex *N*-glycan synthesis is observed only in the subset of CHO cells expressing a sufficiently high level of MGAT4D-L (5). Thus, to demonstrate inhibition of MGAT1 activity in transfectants, it is necessary to sort for *Mgat4d-L* transfectants in which complex *N*-glycan synthesis is clearly inhibited. This is achieved by sorting for transfectants with the highest binding of a lectin that recognizes oligomannosyl *N*-glycans such as GNA (5). We previously demonstrated that *Mgat4d-L* transfectants sorted for high GNA binding exhibit a correspondingly high degree of inhibition of MGAT1 GlcNAc-transferase activity (5). The binding profile for GNA may therefore be used to determine the inhibitory activity of transfectants expressing mutant *Mgat4d-L*. The basis of the assay is illustrated in Fig. 1*A*. Sugar symbols conform to the recommendations of the Symbol Nomenclature for Glycans (9, 10). *Mgat4d-L*–transfected CHO cells selected for hygromycin resistance were examined by flow cytometry for GNA binding and GNA-high and -low populations were identified (Fig. 1*B*). Sorting for GNA-high transfectants gave a population of cells with increased binding of GNA (Fig. 1*C*) and expression of MGAT4D-L based on Western blotting analysis (Fig. 1*D*), as expected if inhibition of MGAT1 caused increased expression of oligomannosyl *N*-glycans that bind GNA.

MGAT4D-L inhibits Drosophila MGAT1

The *Mgat4d* gene is expressed highly in testicular germ cells, and at basal levels in other mouse tissues (5). Thus, most mammalian cell lines do not express *Mgat4d-L*, and there is no homologue in *Drosophila* (BLASTn mouse *Mgat4d-L* accession No. HM067443.1 *versus Drosophila* RefSeq RNA). To determine whether mouse MGAT4D-L inhibits *Drosophila* MGAT1 in the nonmammalian context of *Drosophila* cells, S2R+ adherent cells carrying an inactivating mutation in the gene-fused lobes (*fdl*), which encodes a hexosaminidase that removes the GlcNAc transferred by MGAT1 to $Man_5GlcNAc_2Asn$ (11, 12), were used. S2R+ cells were transfected with a bicistronic *pAc5-STABLE2-Neo* vector (13) encoding mouse *Mgat1* and mCherry, or mouse *Mgat4d-L* and eGFP as bicistrons, respectively. Transfectants resistant to G418 were analyzed for eGFP

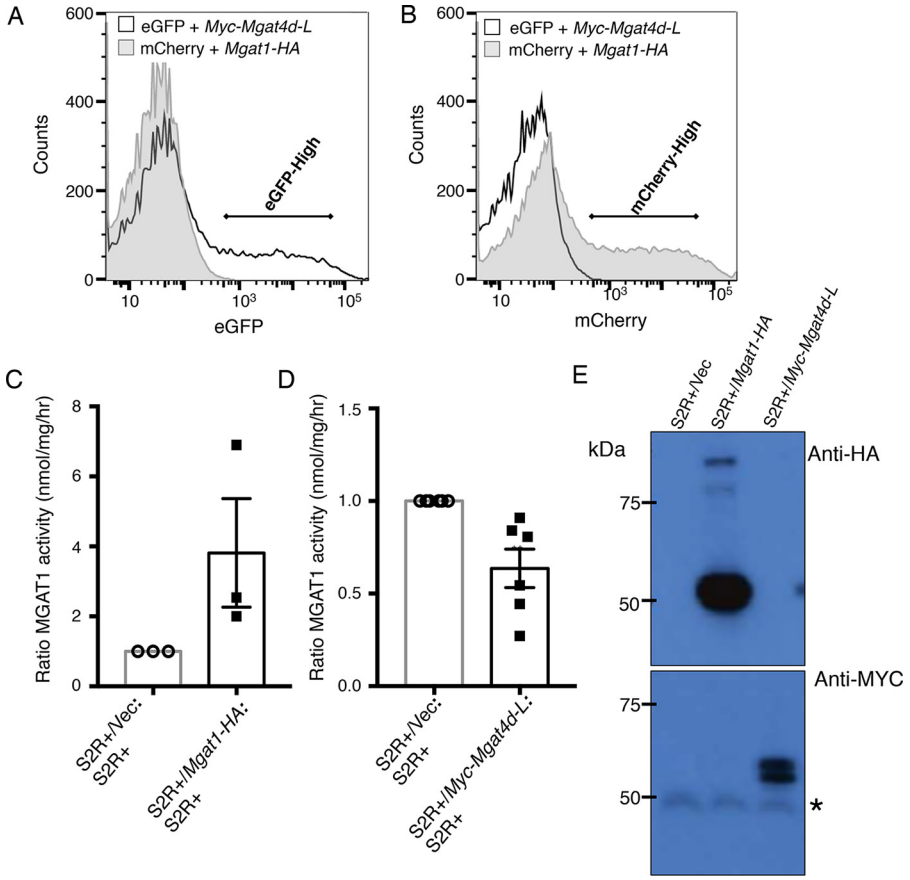

Figure 2. Inhibition of *Drosophila* MGAT1 by mouse MGAT4D-L. *A* and *B,* representative flow cytometry profiles of S2R+ Dm*fdl* cells transfected with pAc5 bicistronic vector encoding eGFP and *Myc-Mgat4d-L* or mCherry and *Mgat1-HA*. *C,* MGAT1 activity in S2R+ Dm*fdl* cells transfected with empty vector (control) compared with S2R+ Dm*fdl* cells transfected with mCherry + *Mgat1-HA* (bicistron). The ratio of MGAT1 activities were determined as indicated. MGAT1 activity in S2R+/Vec lysates was 2.46 ± 0.71 (mean ± S.E.) nmol/mg protein/h ($n = 6$). *D,* the ratio of MGAT1 activity in S2R+/empty vector lysate to S2R+ cells and S2R+/*Myc-Mgat4d-L* to S2R+ cells. *E,* Western blotting of S2R+ Dm*fdl* transfectant lysates. MGAT1-HA was detected using anti-HA antibodies and MYC-MGAT4D-L was detected using anti-MYC antibodies. * identifies a nonspecific band that serve as loading control.

or mCherry expression by flow cytometry (Fig. 2, *A* and *B*). It can be seen that the expression level of eGFP and mCherry varied broadly across the population of transfectants, reflecting similarly varying levels of MGAT1 and MGAT4D-L in these populations. Cell lysates from each transfectant population were assayed for MGAT1 activity (Fig. 2, *C* and *D*). Attempts to purify eGFP- or mCherry-high subpopulations were not successful because of the low viability of S2R+ Dm(*fdl*) cells after sorting. Transfection of S2R+ Dm*fdl* cells with mouse *Mgat1-HA* resulted in a predictable increase in MGAT1 activity (Fig. 2*C*). Moreover, transfection with Myc-*Mgat4d-L* caused a reduction in endogenous *Drosophila* MGAT1 activity, compared with cells transfected with empty vector (Fig. 2*D*). Both *Mgat1* and *Mgat4d-L* transgenes were well-expressed in the respective transfectant populations (Fig. 2*E*). The relatively modest reduction in endogenous MGAT1 activity probably reflects the large variation in expression of MGAT4D-L observed in the broad range of eGFP expression in transfectants (Fig. 2*B*). Thus, MGAT4D-L inhibited *Drosophila* MGAT1, which is ~59% identical to mouse MGAT1. This suggests that the presence of mammalian Golgi factor(s), or a particular enzyme complex such as the "kin recognition" complex (14, 15), are not essential for MGAT4D-L to inhibit MGAT1 (6). However, mammalian factors in the secretory pathway may promote inhibitory activity.

Mutational analysis of MGAT4D-L

We previously showed that deletion of the C-terminal 39 aa of MGAT4D-L inactivates its MGAT1-inhibitory activity (5). To refine that analysis, we sequentially deleted 20, 25, 30, and 35 aa from the C terminus of MYC-MGAT4D-L (Fig. 3*A*). CHO transfectants were selected for resistance to hygromycin and shown to express the relevant MYC-MGAT4D-L mutant protein at a level at least equivalent to control WT protein (Fig. 3*B*). Flow cytometry for GNA binding showed that removal of 25 or more amino acids led to inactivation of MYC-MGAT4D-L, whereas removal of 20 aa did not (Fig. 3*C*). The five critical amino acids were ^{393}PSLFQ^{397}. Further mutations were made to investigate roles for PSLFQ in MGAT4D-L (Fig. 4*A*). Western blot analysis of CHO transfectants expressing vector control or different mutant constructs showed robust expression (Fig. 4*B*). Conversion of PSLFQ to AAAAA in the context of full-length MYC-MGAT4D-L resulted in an inactive MGAT4D-L that did not induce a GNA-high population of transfectants (Fig. 4*C*). The same result was obtained when

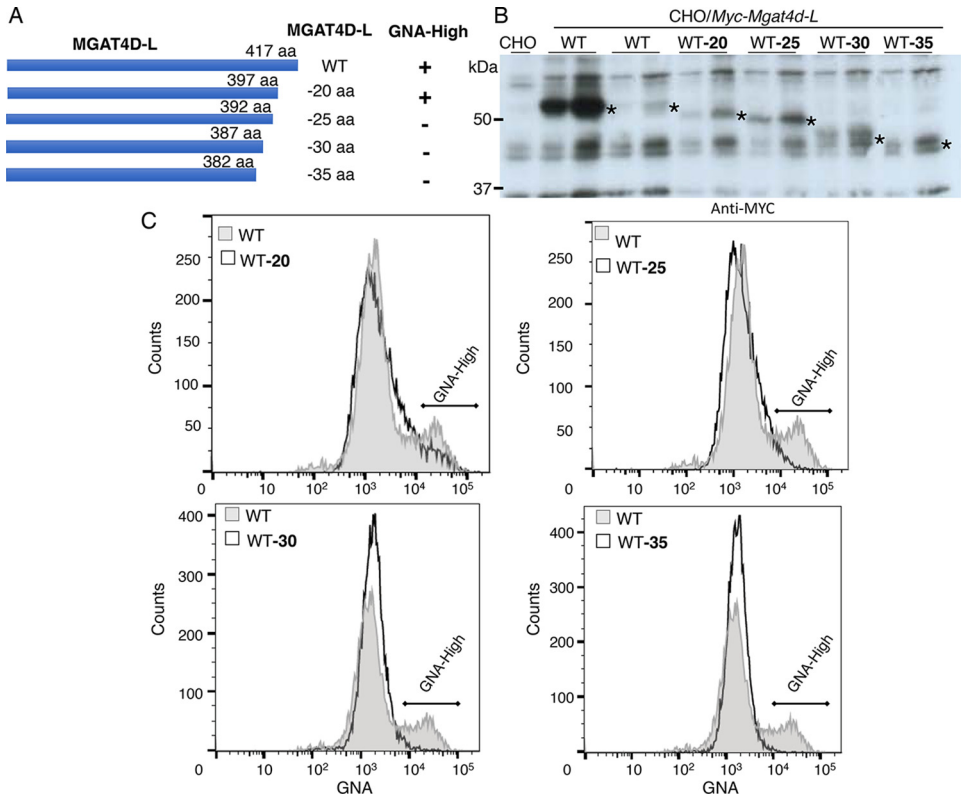

Figure 3. C-terminal deletion analysis of MGAT4D-L. *A,* schematic representation of MGAT4D-L (*WT*) and deletion mutants (WT-20, WT-25, WT-30, and WT-35) and the GNA-binding ability of transfectants expressing each construct. *B,* Western blotting of lysates from CHO cells transfected or not (CHO) with *Myc-Mgat4d-L* WT or each deletion mutant (20 and 40 μg of lysate analyzed for each sample). The first WT pair were from a separate transfection. MYC-MGAT4D-L (*) was detected using anti-MYC antibodies. *C,* representative flow cytometry profiles from CHO cells transfected with MGAT4D-L deletion mutants as labeled.

PSLFQ was deleted from the full-length molecule (Fig. 4*D*). Finally, if 25 aa were removed and AAAAA was added in place of PSLFQ, the resulting MGAT4D-L mutant was also unable to induce a GNA-high population of transfectants (Fig. 4*E*), in contrast to the control WT-20 that terminates in PSLFQ (Fig. 3*C*). Importantly, these changes to the MYC-MGAT4D-L sequence did not prevent the interaction of MGAT4D-L mutants with MGAT1. Thus, co-immunoprecipitation (IP) of WT *versus* mutant or truncated MYC-MGAT4D-L with MGAT1-HA gave a similar IP signal (Fig. 4*F*). By contrast, control, untransfected lysate or co-transfection of MYC-MGAT4D-L with an unrelated protein (HA-p85ni), gave no co-immunoprecipitation signal (Fig. 4*F*).

MGAT4A and MGAT4B do not inhibit MGAT1

Two glycoproteins related to MGAT4D-L, termed MGAT4A and MGAT4B, are membrane-bound, Golgi GlcNAc-transferases, and also contain a PSLFQ sequence (Fig. S1). We therefore investigated whether transfection of either of these cDNAs into CHO cells inhibited MGAT1. Full-length human *MGAT4A* and *MGAT4B* cDNAs were cloned following reverse transcription of HL-60 cell RNA, and shown to have the same nucleotide sequence as GenBank accession numbers AB000616.1 and AB000624.1, respectively (16, 17). We transfected each cDNA or empty vector into a CHO cell line stably expressing human *FUT4* (CHO/*FUT4*), which causes complex *N*-glycans to carry α1,3Fuc on Galβ1,4GlcNAc (*N*-acetyllactosamine or LacNAc) sequences in the branches of complex *N*-glycans (18). The resulting Galβ1,4(Fucα1,3)GlcNAc epitope is termed Lewis X (LeX). The LeX determinant cannot be synthesized on *N*-glycans in a cell lacking MGAT1 because there would be no LacNAc-containing branches (19), and thus no substrate for FUT4. CHO/*FUT4* cells overexpressing human *MGAT4A* or *MGAT4B* were shown to be highly resistant to the toxicity of pea lectin (PSA) (Table 1), proving that both transferases were active and reduced the complement of complex *N*-glycans recognized by PSA, presumably by inhibiting binding to the fucosylated *N*-glycan core due to increased branching of this core (20). LEC18 CHO cells were used as a positive control (21). Resistance to PSA is also observed in Lec1 CHO cells or CHO/*Mgat4d-L* cells in which MGAT1 is inactive (5, 6, 22). By contrast, the *MGAT4A* and *MGAT4B* transfectants expressed LeX similarly to CHO/*FUT4* control cells (Table 1). LEC12 CHO cells, which express LeX due to expression of the *Fut9* gene (23), were used as a positive control. This shows that *MGAT4A* or *MGAT4B* transfection did not inhibit MGAT1 activity because, in CHO cells, LeX is present only on LacNAc sequences in complex *N*-glycan branches (19). Further evidence that MGAT4A or MGAT4B did not inhibit MGAT1 was obtained by lectin-binding and lectin-resistance experiments. CHO/*FUT4*/*MGAT4A* and CHO/*FUT4*/*MGAT4B* transfectants, before or after treatment with sialidase to remove sialic acid from cell surface glycans, were incubated with fluorescein isothiocyanate (FITC)-conjugated *Ricinus communis* agglutinin I or II (RCAI-FITC, RCAII-FITC), or wheat germ agglutinin

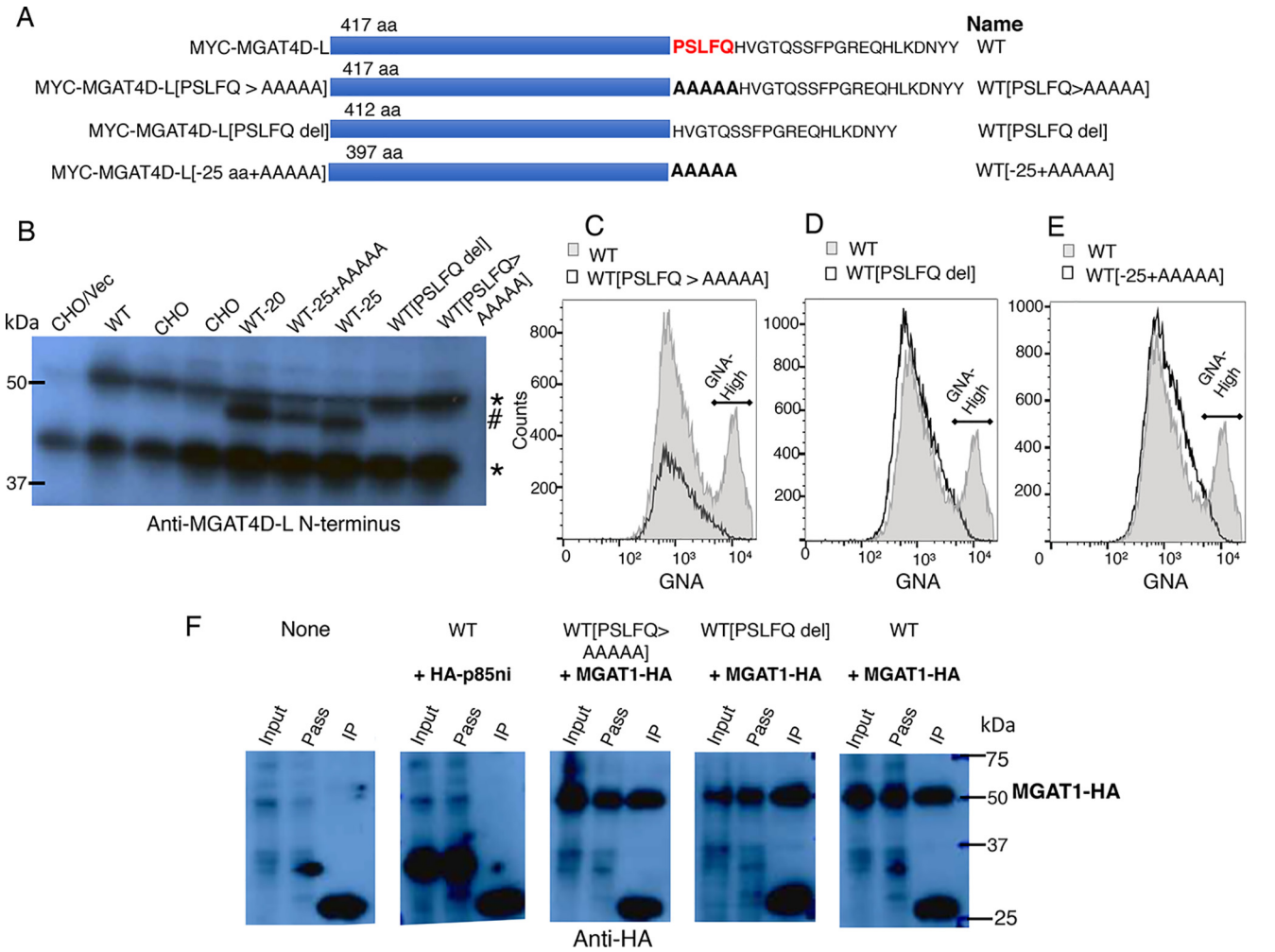

Figure 4. Mutational analysis of MGAT4D-L. *A,* schematic presentation of MYC-MGAT4D-L (*WT*) and different mutants expressed in CHO transfectants. *B,* Western blotting of lysates from transfectants expressing constructs described in *A*, whose flow cytometry profiles are shown in *C–E*. The blot was probed with pAb to the N terminus of MGAT4D-L. WT corresponds to WT in *panels C–E*. # marks MGAT4D-L species; * marks nonspecific bands. The nonspecific band that runs slightly higher than MGAT4D-L (WT) and full-length mutant WT[PSLFQ>AAAAA] is distinguished by its comparatively low expression in empty vector transfectant (*CHO/Vec*) and its presence in the two lanes with CHO lysate. *C–E,* representative GNA flow cytometry profiles of CHO cells transfected with the MYC-MGAT4D-L mutants described in *A* compared with a WT control repeated in each panel. The profiles for each mutant are slightly skewed due to the voltage and gating used. *F,* CHO cells co-transfected with *Myc-Mgat4d-L* or a *Myc-Mgat4d-L* mutant and *Mgat1-HA* or negative control *HA-p85ni* were lysed, incubated with beads conjugated to anti-MYC antibodies, washed, and bound proteins eluted from the beads were subjected to SDS-PAGE as described under "Experimental procedures." Western blotting was performed with anti-HA antibodies to detect co-immunoprecipitated HA-tagged protein. Only samples with co-transfected MYC-MGAT4D-L and MGAT1-HA had a signal corresponding to co-immunoprecipitated MGAT1-HA (*IP lane*). *Input* and *Pass* (unbound) show that MGAT1-HA was robustly expressed in co-transfectants. The negative control HA-p85ni was not immunoprecipitated by anti-MYC beads as expected.

(WGA-FITC), and analyzed by flow cytometry. Each of these lectins binds to complex *N*-glycans–RCAI and RCAII bind Gal residues and WGA binds sialic acid in complex *N*-glycans (24). *MGAT4A* and *MGAT4B* transfectants bound RCAII-FITC similarly to vector control before sialidase treatment (Fig. S2). After sialidase treatment, binding to *MGAT4A* and *MGAT4B* transfectants was increased relative to CHO/vector, consistent with the exposure of Gal residues on an increased number of complex *N*-glycan branches stemming from the action of *MGAT4A* or *MGAT4B* (Fig. S2). The results for WGA were similar (Table 1). In addition, transfectants were tested for resistance to the toxicity of RCAII, WGA, and concanavalin A (ConA). CHO cells expressing complex *N*-glycans are ~90% killed by ~4 ng/ml of RCAII, or ~5 μg/ml of WGA, or ~15 μg/ml of ConA (22). The concentration of each lectin that gave ~90% killing of CHO/*FUT4*/Vec, CHO/*FUT4*/*MGAT4A*, or CHO/*FUT4*/*MGAT4B* was similar in each case. If MGAT1 activity was inhibited by *MGAT4A* or *MGAT4B* overexpression, transfectants would have been highly resistant to WGA, and hypersensitive to the toxicity of ConA, as observed in CHO/*Mgat4d-L* transfectants in which MGAT1 is inhibited (5), and in Lec1 CHO cells (22). Therefore, neither *MGAT4A* nor *MGAT4B* inhibited MGAT1 activity when overexpressed in CHO/*FUT4* cells.

Transfer of inhibitory activity to MGAT1 chimeric proteins

To determine whether PSLFQ or the 25-aa C terminus of MGAT4D-L could be sufficient to inhibit MGAT1 when expressed on a scaffold protein, we examined the inhibitory activity of chimeras comprising membrane-bound MGAT1 extended with a C-terminal peptide from MGAT4D-L. MGAT1 was investigated as a scaffold because it forms

Table 1

Characterization of CHO/*FUT4* cells expressing *MGAT4A* or *MGAT4B*

The first column gives the % cells in the designated population (Pop) or clones derived from a single cell by limiting dilution, which bound Ab against the LeX epitope. Cells were grown on glass slides and binding of primary Ab was determined using FITC-conjugated secondary Ab by immunofluorescence microscopy, as described under "Experimental procedures." The next two columns give the concentration of PSA or RCAII lectin that resulted in 10% survival (D_{10}) or 90% death of transfectant cell populations, or stable clones, as shown. The last two columns give the mean fluorescence index (MFI) for WGA-FITC or RCAI-FITC binding to transfectant cell populations. Removal of sialic acid by sialidase caused decreased binding of WGA, consistent with the loss of sialic acid from complex *N*-glycans. By contrast sialidase treatment caused the binding of RCAI to increase, consistent with the exposure of Gal residues in complex *N*-glycans. The increase was greater for CHO/*FUT4* cells expressing *MGAT4A* or *MGAT4B*, consistent with increased complex *N*-glycan branching in those transfectants. Empty cells signify the assay was not performed. These experiments were performed in another context, long before development of the GNA-binding assay.

Cells	LeX	PSA		RCAII	MFI WGA		MFI RCAI	
	Binding (%)	*D_{10} (μg/ml)*		*D_{10}(ng/ml)*	*Sialidase*[a]			
	Pop	Pop	Clone	Clone	−	+	−	+
CHO	0	~100	~100	10				
CHO/*FUT4*/vector	70	~100	~100	~4	38	10	63	191
CHO/*FUT4/MGAT4A*	70	~1000	~1000	~4	27	9	49	237
CHO/*FUT4/MGAT4B*	80	~300	~1000	~4	38	10	75	221
LEC12	100			~4				
LEC18		>1000	> 1000	10				

[a]The − and + signs refer to untreated (−) or treated (+) with sialidase.

homomers in the Golgi (6). We generated a CHO *Myc-Mgat1* cDNA with the MYC tag on the N terminus, and used this construct to make the following chimeras: *Myc-Mgat1*[+25aa] (to produce MYC-MGAT1 terminating in the last 25 aa of MGAT4D-L), *Myc-Mgat1*[+AAAAA + 20aa] (to produce MYC-MGAT1 with 5 Ala in place of PSLFQ in the last 25 aa of MGAT4D-L), *Myc-Mgat1*[+PSLFQ] (to produce MYC-MGAT1 with ^{393}PSLFQ^{397} at the C terminus), and *Myc-Mgat1* [+AAAAA] (to produce MYC-MGAT1 with 5 Ala residues at its C terminus) (Fig. 5*A*).

The MGAT1 chimeric constructs were transfected into Lec1 CHO cells that lack MGAT1 activity (25). Transfected cells were selected for resistance to hygromycin, harvested, fixed, and analyzed for GNA binding by flow cytometry (Fig. 5, *B* and *C*). All chimeric constructs were well-expressed in transfectant populations. (Fig. 5*D*). Based on signals from nonspecific bands, *Myc-Mgat1*[+PSLFQ] was expressed in more cells, or more highly, than *Myc-Mgat1*[+AAAA]. However, *Myc-Mgat1* [+AAAAA+20aa] and *Myc-Mgat1*[+25aa] were expressed at a similar level. Transfection of *Mgat1* into Lec1 cells generated two major populations, one with low GNA binding due to MGAT1 expression leading to the synthesis of complex *N*-glycans, and the other in which *Mgat1* transgene expression was weak or absent and did not change the high GNA binding of Lec1 cells. The expected result for transfectants expressing chimeric MGAT1 with completely inhibited activity was no reduction in GNA binding; partial inhibition of MGAT1 should have given a small reduction in GNA binding; and a chimera with no inhibition of MGAT1 should give a low GNA-binding population reflecting active MGAT1. In fact, the appearance of a population with an intermediate GNA-binding phenotype reflecting partial MGAT1 inhibition, was observed in *Myc-Mgat1* [+PSLFQ] and *Myc-Mgat1*[+25aa] transfectants, but not in their respective controls expressing *Myc-Mgat1*[+AAAAA] or *Myc-Mgat1*[+AAAAA+20aa] (Fig. 5, *B* and *C*). Although the intermediate GNA-binding population was modest, the result was reproducible, and this change was the most readily quantitated. In summary, the results show that MGAT1 terminating with either the critical amino acids PSLFQ, or the last 25 aa of MGAT4D-L (including PSLFQ), caused a partial inhibition of MGAT1 activity, either due to *cis*-inhibition of MGAT1 chimera or to *trans*-inhibition in MGAT1 homooligomers formed in the Golgi (6, 26). To pursue this chimeric strategy further, optimization of terminal peptide composition would be necessary.

Two point mutations independently inactivate MGAT1 inhibition by MGAT4D-L

To address the importance of each amino acid in the sequence critical for MGAT4D-L inhibitory activity (PSLFQ), point mutations were performed to change each amino acid in turn to Ala in the *Myc-Mgat4d-L* plasmid. *Myc-Mgat4d-L* with AAAAA in place of PSLFQ was used as a negative control. The constructs were transfected into parental CHO cells, and transfectants selected for resistance to hygromycin were shown to express levels of mutant MYC-MGAT4D-L protein higher than WT control (Fig. 6*A*). Flow cytometry analysis of GNA binding revealed that changing Pro-393, Ser-394, or Gln-397 to Ala did not abolish the MGAT1 inhibitory activity of MYC-MGAT4D-L (Fig. 6*B*). By contrast, changing Leu-395 or Phe-396 to Ala significantly impaired the ability of MYC-MGAT4D-L to inhibit MGAT1, as shown by the absence of a GNA-high transfectant population (Fig. 6*B*). To determine whether MYC-MGAT4D-L with an inactivating point mutation was localized to the Golgi compartment where MGAT4D-L inhibits MGAT1 (6), we performed confocal microscopy on HeLa cell transfectants. Co-localization experiments with the Golgi resident protein GM130 revealed that mutated and WT MYC-MGAT4D-L were co-localized in the Golgi (Fig. 7). In 15 transfected cells per construct, 79% of WT MYC-MGAT4D-L transfectants showed complete and 21% partial colocalization of MGAT4D-L with GM130. The mutant constructs exhibited 65 and 77% complete with 35 or 23% partial co-localization with GM130, for L395A or F396A, respectively. Therefore, both inactivating point mutants of MYC-MGAT4D-L were well localized to the Golgi compartment, but did not inhibit MGAT1.

Discussion

In this paper we identify features of MGAT4D-L important for inhibiting MGAT1. We show that mammalian MGAT4D-L inhibited *Drosophila* MGAT1 activity in S2 cells, indicating that a mammalian Golgi environment is not essential for inhibition to occur. However, the inhibition was modest, which may reflect the mixed transfectant population or may indicate that a mammalian Golgi environment better facilitates inhibition of MGAT1 by MGAT4D-L.

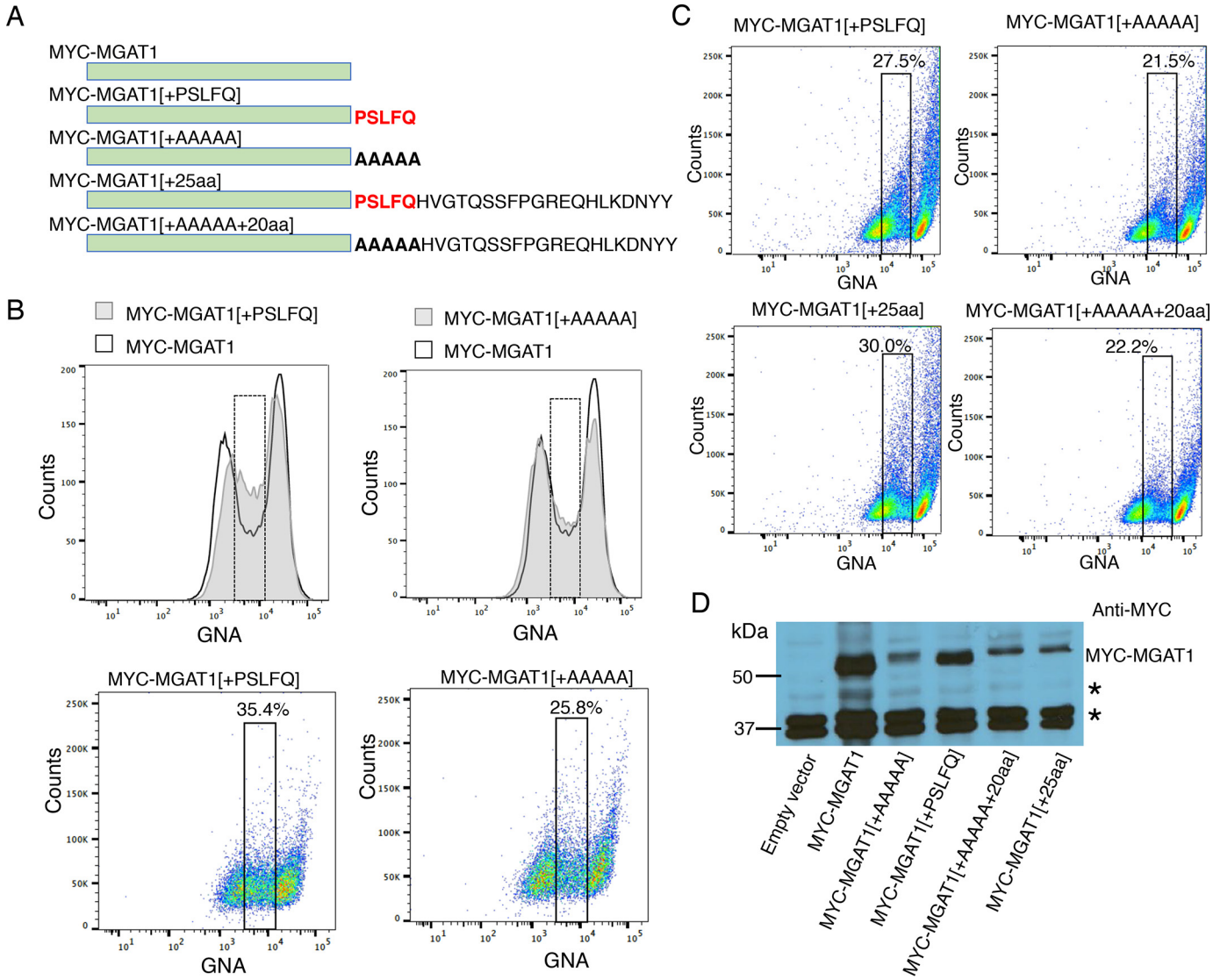

Figure 5. PSLFQ at the MGAT1 C terminus partially inhibits MGAT1 activity. *A,* schematic representation of MYC-MGAT1-MGAT4D chimeric proteins. MYC-MGAT1 was fused at the C terminus with PSLFQ or AAAAA, or the last 25 aa of the MGAT4D C terminus including PSLFQ, or the last 25 aa of MGAT4D C terminus but with AAAAA in place of PSLFQ. *B, top panels*: flow cytometry profiles of Lec1 CHO cells that lack MGAT1 activity transfected with *Myc-Mgat1 versus Myc-Mgat1[PSLFQ]* (*left*) or *Myc-Mgat1 versus Myc-Mgat1[AAAAA]* (*right*). The *rectangle with dotted lines* highlights the intermediate GNA-binding subpopulation. *Bottom panels*, dot plot presentation of data for chimeric MYC-MGAT1 proteins from the *top panels*. *C, top panels*: independent experiment of the same chimeric MYC-MGAT1 proteins shown in *B*. *Bottom panels*: flow cytometry dot plot of Lec1 CHO cells expressing MYC-MGAT1 with 25 C-terminal aa of MGAT4D (*left*) or MYC-MGAT1 with AAAAA + 20 C-terminal aa of MGAT4D. *D,* representative Western blotting of lysates from Lec1 transfectants used for flow cytometry analysis, as labeled. Chimeric proteins migrated slower than MYC-MGAT1. * identifies nonspecific bands that serve as loading control.

We used deletion analysis of MGAT4D-L to identify PSLFQ at aa 21-25 from the MGAT4D-L C terminus as necessary for MGAT4D-L to inhibit MGAT1. Replacement with AAAAA or deletion of PSLFQ in the full-length protein led to inactive MGAT4D-L. Importantly, the same 5-aa sequence found in MGAT4A and MGAT4B did not confer MGAT1 inhibitory activity on either of these GlcNAc-transferases. Interestingly, transfer of PSLFQ alone, or the terminal 25 C-terminal amino acids of MGAT4D-L, to the C terminus of MGAT1 conferred partial inhibitory activity on the MGAT1 chimeric protein. The effect was modest but reproducible, and suggested that it might be possible to develop an optimized peptide inhibitor of MGAT1. The combined information from mutational analysis, including the fact that either of the two adjacent amino acids Leu or Phe in PSLFQ are essential for the MGAT1 inhibitory activity of MYC-MGAT4D-L, will be most useful in guiding structural analyses to reveal the mechanism of inhibition in MGAT1–MGAT4D-L complexes, as well as the search for a small molecule inhibitor of MGAT1.

Identifying a small molecule inhibitor of MGAT1 would be most beneficial to basic research on the functions of *N*-glycans in different cell types, and for glycosylation engineering of antibodies and other therapeutics. MGAT1 is a key GlcNAc-transferase because it initiates the synthesis of two major classes of *N*-glycans, hybrid and complex (reviewed in Ref. 7). If MGAT1 is inactivated, a cell can express only oligomannosyl *N*-glycans on its complement of glycoproteins (19). This markedly changes the properties of the cell in terms of recognition by

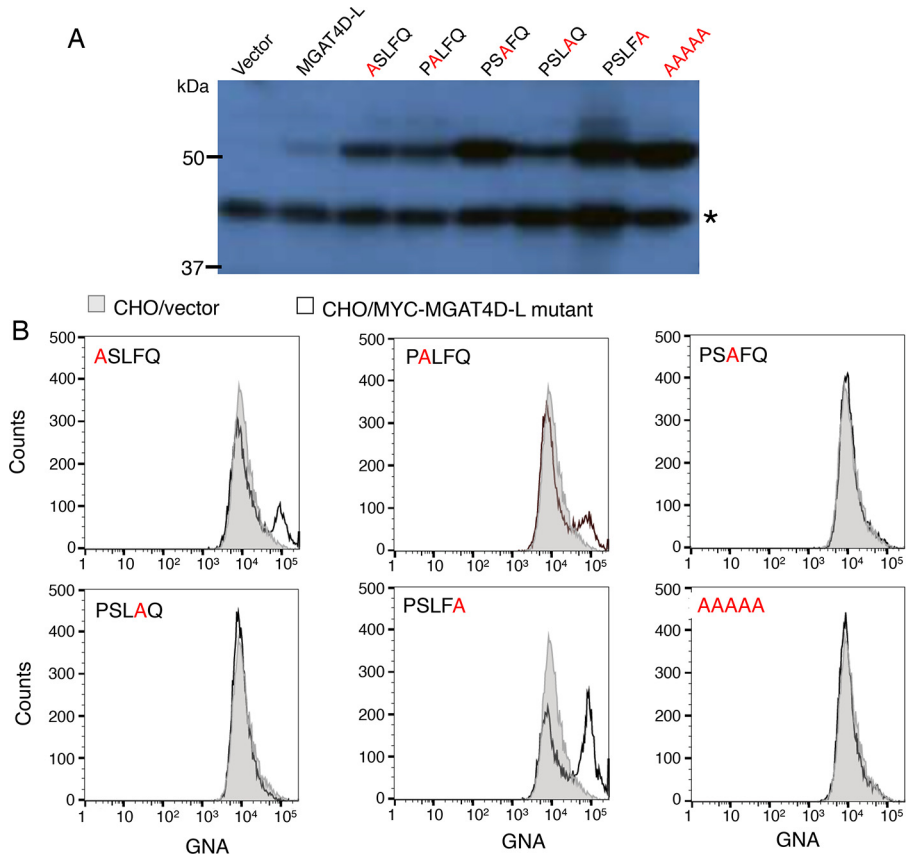

Figure 6. Point mutations that inactivate MGAT4D-L inhibitory activity. *A,* Western blotting analysis of lysates from CHO cells and CHO cells expressing MYC-MGAT4D-L point mutants. 60 μg of cell extract was loaded per lane. MYC-MGAT4D-L was detected with an antibody directed against the MGAT4D-L N terminus. * identifies nonspecific bands that serve as loading control. *B*, representative flow cytometry profiles of GNA binding to CHO cells transfected with MGAT4D-L point mutants.

glycan-binding proteins, antibodies, and organisms that can infect. Loss of *Mgat1* in embryogenesis leads to death at embryonic day (E) E9.5 (27, 28). Loss from spermatogonia at 3 days after birth leads to a failure of spermatogenesis and infertility (29, 30). Loss of complex *N*-glycans from CHO cells causes them to respond poorly to growth factors that stimulate extracellular signal-regulated kinase signaling (31). Removal of MGAT1 activity from CHO cells synthesizing IgG leads to the production of antibodies with enhanced antigen-dependent cellular cytotoxicity (32). Generation of glycoproteins in cells lacking MGAT1 often enhances their ability to form crystals for X-ray crystallography (33). Thus, the availability of an inhibitor of MGAT1 that could be readily used to manipulate the synthesis of complex *N*-glycans in cells and organisms is highly desirable. The discovery of features of the Golgi glycoprotein MGAT4D-L required for inhibition of MGAT1 (5, 6) opens a path to this goal.

Experimental procedures

Plasmids

The expression construct previously termed *Myc-GnT1IP-L* in pcDNA3.1-Hygro(+) (6) and now *Myc-Mgat4d-L* was used to generate different mutant versions of *Mgat4d-L* using the End Point PCR, Gibson Assembly NEBuilder HiFi DNA Assembly Cloning Kit (E5520, New England Biolabs, Ipswich, MA). Site-directed mutagenesis was performed using the Q5 site-directed mutagenesis kit (New England Biolabs, E0554). The construct *Mgat1-HA* in pcDNA 3.1-Hygro(+), described previously (6), was used for the generation of different chimeric MYC-MGAT1 proteins. Ac5-STABLE2-neo plasmid containing an insect expression cassette was from Addgene (plasmid 32426; Addgene_32426). End point PCR and insert ligation were used to generate the bicistronic constructs mouse *Myc-Mgat4d-L*-T2A-eGFP and mCherry-T2A-mouse *Mgat1-HA*. Primers used in generating *Mgat4d-L* and *Mgat1* constructs are given in Table S1.

Human *MGAT4A* and *MGAT4B* were cloned into pZeoSV2 (+) from cDNA generated from HL-60 cell RNA. RNA was isolated from HL-60 cells using TRIzol (Invitrogen) following the manufacturer's instructions. Reverse transcription was performed using random hexamers and the SuperScript II kit (Invitrogen). *MGAT4A* and *MGAT4B* cDNAs were amplified using the following primers *MGAT4A,* PS301 (Fwd) 5'-tccgc**ggtacc**accatgaggctccgcaatggaact containing a Kozak sequence and KpnI restriction site (bolded), and PS302(Rev) 5'-ta**gggccc**tcagatgatcagttggtggc containing an ApaI restriction site (bolded); *MGAT4B* PS337(Fwd) 5'-tcttaa**gaattc**caccatgaggctccgcaatggcacct containing a Kozak sequence and EcoRI restriction site (bolded) and PS338(Rev) 5'-tgggcc**ctcgag**cttagtcggccttttcaggaagat containing a XhoI restriction site (bolded). PCR products were either cloned directly into

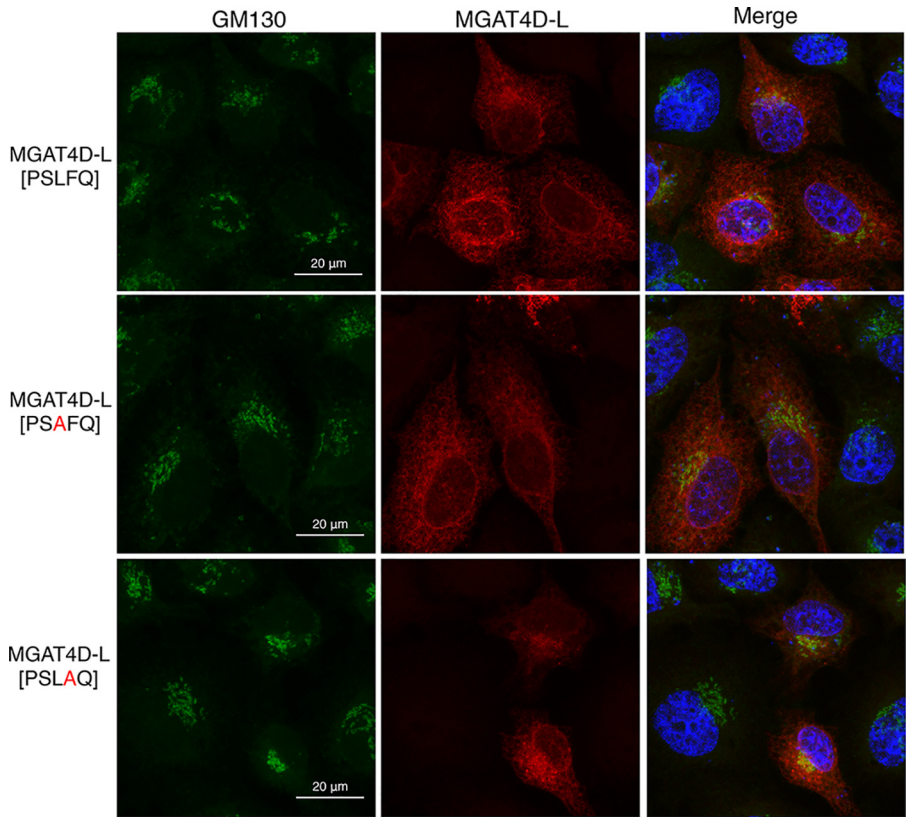

Figure 7. Localization of MGAT4D-L point mutants in the Golgi apparatus. Confocal analysis of HeLa cells transfected with *Myc-Mgat4d-L*, *Myc-Mgat4d-L* (PS**A**FQ), or *Myc-Mgat4d-L*(PSL**A**Q). Primary antibodies directed against the Golgi marker GM130 detected by anti-mouse antibodies conjugated to Alexa 488 define the Golgi compartment (*green*). MGAT4D-L was detected using anti-MGAT4D-L N terminus antibodies detected by anti-rabbit secondary antibody conjugated to Alexa 594 (*red*).

pZeoSV2(+), or first into pCR2.1 and then restriction digested products were cloned into pZeoSV2(+). Plasmids were purified using Qiagen plasmid kits (Qiagen, Hilden, Germany). The sequence of each construct was determined and validated by the Genomics Core of the Albert Einstein College of Medicine. Primers for characterizing *MGAT4A* and *MGAT4B* expression in CHO/*FUT4* transfectants are given in Table S2.

Cell culture and transfection

CHO WT (Pro$^-$5) and Lec1 cells (Pro$^-$5Lec1.3C) were maintained in α-minimal essential medium (Gibco, Grand Island, NY) supplemented with 10% (v/v) fetal bovine serum (Gemini Bio, West Sacramento, CA) and 1% penicillin and streptomycin (Gibco). Cells grown to ~70–80% confluence in a 6-well–plate were transfected with 2 μg of plasmid DNA mixed with X-treme Gene HP DNA transfection reagent (number 06366 244 001, Sigma-Aldrich) at a ratio of 1:3 (DNA:reagent), following the manufacturer's protocol. At 24 h after transfection, the medium was replaced with medium containing 0.6 mg/ml of hygromycin B (number H3274, Sigma-Aldrich). When hygromycin-resistant cells reached confluence, they were trypsinized and re-plated in a 10-cm plate containing medium with hygromycin. At ~80–90% confluence, transfectants were trypsinized, counted, and used to seed roller tubes containing 10 ml of hygromycin medium. At ~6-8 × 10^5 cells/ml (~3 days in culture), cells were harvested for flow cytometry and Western blotting analysis.

Drosophila S2+ Dm*fdl* cells in which the *fdl* gene is deleted (12) were kindly provided by Donald L. Jarvis. The cells were cultured at 28 °C in Schneider's medium (Life Technologies) with 10% (v/v) fetal bovine serum and 1% antibiotic mix in a T25 or T75 flask. Transfection of S2R+ Dm*fdl* cells with plasmids was performed using Lipofectamine (Invitrogen) following the manufacturer's protocol for 2 μg of plasmid. Stably transfected cells were selected using 0.7 mg/ml of active G418 (number 400–111 P, Gemini, Sunnyvale, CA) for up to 14 days before using cells for analysis.

Empty vector or *MGAT4A* or *MGAT4B* cDNA were transfected into CHO/*FUT4* cells (18) using Lipofectamine (Invitrogen) according to the manufacturer's instructions. Stable transfectant populations were obtained by selection with Zeocin (Gibco). Stable clones were obtained by limiting dilution.

Antibodies

Affinity-purified, rabbit anti-MGAT4D-L N terminus peptide polyclonal antibodies (pAb) made by Covance (Denver, PA) have been characterized previously (34); mouse anti-MYC mAb (9E10) and mouse anti-HA mAb (HA.11) were from Covance (Princeton, NJ); secondary Ab for both was goat anti-rabbit IgG (H+L) conjugated to horseradish peroxidase (Thermo Fisher Scientific, Waltham, MA); mouse anti-rat Golgi GM130 mAb was from BD Biosciences (San Jose, CA); secondary antibodies conjugated to Alexa 488 (green; donkey anti-mouse IgG), or Alexa 594 (red; chicken anti-rabbit IgG)

were from Invitrogen Life Technologies. Anti-LeX mAb was from hybridoma 480 provided by Barbara Knowles as described previously (35). Rabbit anti-mouse IgM secondary Ab (number 61-6811) conjugated to FITC was from Zymed Laboratories Inc. (South San Francisco, CA).

Flow cytometry

Flow cytometry was performed as previously described (6). Briefly, ~6×10^6 cells were washed with 10 ml of cation-free PBS at room temperature, fixed in 1 ml of 4% paraformaldehyde in the dark at room temperature for 15 min, washed 3 times with 1 ml of FACS buffer (Hank's balanced salt solution containing 1 mM $CaCl_2$, 1 mM $MgCl_2$, 2% BSA (BSA Fraction V, Sigma-Aldrich) and 0.01% sodium azide) and stored in 1 ml of FACS buffer at 4 °C. For flow cytometry, fixed cells were incubated for 1 h with 16 μg/ml of GNA (number B-1245, Vector Laboratories, Burlingame, CA) conjugated with biotin. The cells were then washed 3 times with 1 ml of FACS buffer and incubated with 4 μg/ml of streptavidin-conjugated to phycoerythrin (number SA-5207, Vector Laboratories) for 30 min. After washing, the cells were resuspended in 500 μl of FACS buffer in a flow cytometry tube. Acquisition was performed using a BD LSR II flow cytometer (BD Biosciences). Analysis of flow cytometry data were performed using FlowJo software (Tree Star Inc., Ashland, OR).

For LeX mAb binding, cells were washed with PBS containing 0.05% Tween 20 (PBS-T), fixed in 1% glutaraldehyde (Sigma-Aldrich) at 37 °C for 1 h, washed with PBS, incubated with 2% BSA in PBS containing the primary antibody (0.5 μg in 50 μl of PBS with 2% BSA) for 1 h at 37 °C, washed, and incubated in secondary Ab conjugated to FITC for 1 h, washed, and examined under a fluorescent microscope. For binding of FITC-conjugated lectins WGA, RCAII, or RCAI (Vector Laboratories), 6×10^6 cells were washed 3 times in PBS lacking cations, resuspended in 6 ml of PBS, and divided between 2 tubes. One tube was kept on ice and the other was incubated at 37 °C with 3 μl of *Clostridiuim perfringens* sialidase (number N-2133; 10 units/ml; Sigma-Aldrich). After 1 h, 2×10^5 cells from both tubes were incubated in 200 μl of PBS containing 2% BSA, 0.01% sodium azide, and 0.2 μg of FITC-lectin, rotated at 4 °C for 1 h, washed with 1 ml of binding buffer, and resuspended in PBS for flow cytometry.

Western blotting analysis

Cultured cells were washed twice with PBS and lysed with a lysis buffer containing 1% IGEPAL-630 (Millipore Sigma), 1% Triton X-100 (Sigma-Aldrich), 0.5% deoxycholate (Sigma-Aldrich), 1% protease inhibitors (number 05892791001; Roche *EASYpack* Protease Inhibitor mixture; Millipore Sigma) for 30 min on ice. The lysate was centrifuged at 5,000 × *g* for 5 min and the supernatant was transferred to a new tube and supplemented with glycerol to a final concentration of 20%. The protein yield was determined using a Bradford Bio-Rad protein assay (Bio-Rad). Protein extract (40 to 80 μg of protein) was loaded on a 10 or 12% SDS-PAGE gel for electrophoresis. Transfer to a polyvinylidene difluoride membrane (100 volts for 1 h) was performed using a transfer buffer containing 25 mM Tris-HCl and 192 mM glycine in 10% methanol. After primary and secondary antibodies incubations, blots were washed 4 times with TBS containing 0.02% Tween 20, followed by 2 times with Tris-buffered saline, and treatment for 5 min at room temperature with Super Signal West Pico PLUS followed in some cases by Femto chemiluminescent substrate (ThermoFisher). Excess reagent was removed and the blot exposed to X-ray film (USA Scientific, Ocala, Florida) for various times.

MGAT1 assay

Cells extracts, prepared as described above in a mixture of detergents in the presence of protease inhibitors, were assayed for MGAT1 activity as described previously (5, 6). Briefly, cell extract containing ~40 μg of protein was incubated in the presence of 30 μg of $Man_5GlcNAc_2Asn$ (36) in 62.5 mM MES, pH 6.25, containing 25 mM $MnCl_2$ and 0.75 mM UDP-6H^3-GlcNAc (~6000-10,000 cpm/nmol; PerkinElmer Life Sciences), in a volume of 40 μl, for 2 h at 37 °C. Each reaction was stopped by adding 1 ml of cold ConA buffer (0.1 M sodium acetate, 1.0 M NaCl, 10 mM $MgCl_2$, 10 mM $CaCl_2$, 10 mM $MnCl_2$, and 0.02% sodium azide). After a brief centrifugation, the supernatant was added to a small column of ConA-Sepharose, the column was washed with ConA buffer and products bound to the column were eluted with ConA buffer containing 200 mM α-methylmannoside (Sigma). Elutate was counted in a Beckman scintillation counter and specific activity was calculated as nanomole/mg of protein/h with, compared to without, acceptor substrate.

Immunoprecipitation

Immunoprecipitation was performed as described previously (5) with some modifications. Briefly, anti-Myc mAb (9E10) was conjugated to Protein G Plus-agarose (number 22851; Thermo Fisher) according to the manufacturer's instructions. CHO cells were co-transfected with *Myc-Mgat4d-L* and different plasmids encoding HA-tagged MGAT1 or p85Ni. Cells were harvested 17 h after transfection, washed with normal saline, and lysed in RIPA buffer (number 20-188; Millipore) supplemented with 0.1% SDS and protease inhibitors (number 05892791001; Roche Millipore Sigma) for 30 min at 4 °C. The lysate was centrifuged at 10,000 × *g* for 5 min and the supernatant was diluted in glycerol to a final concentration of 20% glycerol. The protein concentration was measured and 600 μg of lysate protein was used for immunoprecipitation. Each lysate was precleared with 50 μl of lysis buffer-washed Protein G Plus-agarose beads at 50% slurry for 2 h at 4 °C and incubated with 50 μl of anti-Myc–conjugated agarose beads overnight at 4 °C. After centrifugation to pellet the agarose beads, the supernatant (designated pass) was kept, and the beads were washed 4 times with 1 ml of lysis buffer and resuspended in 25 μl of cation-free PBS. The washed beads in 50 μl (50% slurry) were incubated with 10 μl of 6× SDS-PAGE gel sample buffer for 10 min at 90 °C and centrifuged to remove beads. The supernatant was termed IP. Approximately 24 μl of IP was loaded onto a 12% SDS-PAGE gel along with 30 μg of input lysate and an equivalent volume of sample that did not bind to the beads (pass through). Western blotting analysis was performed using anti-HA mAb clone

16B12 (number 901513; Biolegend, San Diego, CA) as described above.

Confocal microscopy

HeLa cells were seeded in 12-well–plates containing poly-L-lysine–coated coverslips (Electron Microscopy Sciences, Hatfield, PA). After 24 h, the cells were transfected with ~1 μg of the indicated plasmid using X-treme gene transfection reagent (Roche, Basel, Switzerland), and incubated for 24 h in a 5% CO_2 incubator at 37 °C. The cells were washed twice with PBS (no cations) and fixed in 4% paraformaldehyde for 15 min. The wells were washed twice with PBS and stored at 4 °C with PBS containing 0.05% sodium azide until use. For immunofluorescence, coverslips with transfected cells were transferred to a glass slide. The immunostaining protocol was adapted from Abcam (Immunocytochemistry and Immunofluorescence Protocol). Briefly, cells were permeabilized with PBS containing 0.1% Triton X-100 for 10 min, and washed 3 times with PBS. Nonspecific binding was blocked with 1% BSA and 22.52 mg/ml of glycine in PBST (PBS with 0.1% Tween 20) for 30 min. The cells were incubated for 1 h with primary antibody diluted in PBST containing 1% BSA, and washed 3 times with PBS. Secondary antibody conjugated to fluorophore was diluted in 1% BSA with PBS and incubated for 1 h with cells in the dark. The cells were washed 3 times with PBS and incubated 1 min with 0.5 μg/ml of Hoechst dye 33342 (Molecular Probes, Eugene, OR). Coverslips were mounted on a microscope slide using ProLong Diamond Antifade mounting media (number P36961, Molecular Probes). For two-color immunostaining, both primary and then both secondary antibodies were mixed together before being added to the cells. Images were acquired using confocal microscope Leica SP8 (Inverted DMi8) in the Analytical Imaging Facility of Albert Einstein College of Medicine. Acquired images were processed and analyzed using FIJI software (SCR_002285).

Statistical analysis

Data are shown as mean ± S.E. for ≥2 independent experiments, including replicates as noted. A two-tailed, unpaired, Student's *t* test with Welch's correction was used to determine *p* values with GraphPad Prism 7.0a (GraphPad Software Inc., La Jolla, CA).

Data availability

All data presented in this paper are available in the manuscript or from the authors.

Acknowledgments—We thank Rosa Barrio and James Sutherland for reagents, Donald Jarvis for S2R+ Dm*fdl* mutant cells, and the Flow Cytometry and Analytical Imaging and Genomics Core Facilities of the Albert Einstein Cancer Center, supported in part by the National Cancer Institute Grant PO1 13330.

Author contributions—A. A., J. M., M. A., J. T., and P. S. data curation; A. A., J. M., M. A., and P. S. formal analysis; A. A., J. M., M. A., and J. T. investigation; A. A., J. M., M. A., J. T., S. S., and P. S. methodology; A. A. and P. S. writing-original draft; A. A., J. M., M. A., J. T., S. S., and P. S. writing-review and editing; P. S. conceptualization; P. S. resources; P. S. supervision; P. S. funding acquisition; P. S. project administration.

Funding and additional information—This work was supported by National Institutes of Health NIGMS Grant RO1 GM-105399 (to P. S.) and Einstein Core Facilities funded by National Institutes of Health NCI Grant PO1 NCI-13330 (to I. David Goldman). The content is solely the responsibility of the authors and does not necessarily represent the official views of the National Institutes of Health.

Conflict of interest—The authors declare no conflict of interest related to this work.

Abbreviations—The abbreviations used are: CHO, Chinese hamster ovary; GNA, *Galanthus nivalis* agglutinin; aa, amino acid(s); eGFP, enhanced green fluorescent protein; IP, immunoprecipitation; LeX, Lewis X; RCAI and -II, *Ricinus communis* agglutinin I or II; WGA, wheat germ agglutinin; ConA, concanavalin A; HA, hemagglutinin; Ab, antibody.

References

1. Ju, T., Otto, V. I., and Cummings, R. D. (2011) The Tn antigen-structural simplicity and biological complexity. *Angew. Chem. Int. Ed. Engl.* **50,** 1770–1791 CrossRef Medline
2. Sen, J., Goltz, J. S., Konsolaki, M., Schupbach, T., and Stein, D. (2000) Windbeutel is required for function and correct subcellular localization of the *Drosophila* patterning protein Pipe. *Development* **127,** 5541–5550 Medline
3. Yamaji, T., Nishikawa, K., and Hanada, K. (2010) Transmembrane BAX inhibitor motif containing (TMBIM) family proteins perturbs a trans-Golgi network enzyme, Gb3 synthase, and reduces Gb3 biosynthesis. *J. Biol. Chem.* **285,** 35505–35518 CrossRef Medline
4. Chia, J., Tay, F., and Bard, F. (2019) The GalNAc-T activation (GALA) pathway: drivers and markers. *PLoS ONE* **14,** e0214118 CrossRef Medline
5. Huang, H. H., and Stanley, P. (2010) A testis-specific regulator of complex and hybrid *N*-glycan synthesis. *J. Cell Biol.* **190,** 893–910 CrossRef Medline
6. Huang, H. H., Hassinen, A., Sundaram, S., Spiess, A. N., Kellokumpu, S., and Stanley, P. (2015) GnT1IP-L specifically inhibits MGAT1 in the Golgi via its luminal domain. *Elife* **4,** CrossRef
7. Stanley, P., Taniguchi, N., and Aebi, M. (2017) *N*-Glycans in *Essentials of Glycobiology* (Varki, A, Cummings, R. D., Esko, J. D., Stanley, P., Hart, G. W., Aebi, M., Darvill, A. G., Kinoshita, T., Packer, N. H., Prestegard, J. H., Schnaar, R. L., and Seeberger, P. H., eds) pp. 99–111, Cold Spring Harbor Laboratory, Cold Spring Harbor, NY
8. Au, C. E., Hermo, L., Byrne, E., Smirle, J., Fazel, A., Simon, P. H., Kearney, R. E., Cameron, P. H., Smith, C. E., Vali, H., Fernandez-Rodriguez, J., Ma, K., Nilsson, T., and Bergeron, J. J. (2015) Expression, sorting, and segregation of Golgi proteins during germ cell differentiation in the testis. *Mol. Biol. Cell* **26,** 4015–4032 CrossRef Medline
9. Varki, A., Cummings, R. D., Aebi, M., Packer, N. H., Seeberger, P. H., Esko, J. D., Stanley, P., Hart, G., Darvill, A., Kinoshita, T., Prestegard, J. J., Schnaar, R. L., Freeze, H. H., Marth, J. D., Bertozzi, C. R., *et al.* (2015) Symbol nomenclature for graphical representations of glycans. *Glycobiology* **25,** 1323–1324 CrossRef Medline
10. Neelamegham, S., Aoki-Kinoshita, K., Bolton, E., Frank, M., Lisacek, F., Lutteke, T., O'Boyle, N., Packer, N. H., Stanley, P., Toukach, P., Varki, A., Woods, R. J., and Group, S. D, SNFG Discussion Group, (2019) Updates to the symbol nomenclature for glycans guidelines. *Glycobiology* **29,** 620–624 CrossRef Medline

11. Geisler, C., Aumiller, J. J., and Jarvis, D. L. (2008) A fused lobes gene encodes the processing β-*N*-acetylglucosaminidase in Sf9 cells. *J. Biol. Chem.* **283,** 11330–11339 CrossRef Medline
12. Mabashi-Asazuma, H., Kuo, C. W., Khoo, K. H., and Jarvis, D. L. (2015) Modifying an insect cell *N*-glycan processing pathway using CRISPR-Cas technology. *ACS Chem. Biol.* **10,** 2199–2208 CrossRef Medline
13. González, M., Martín-Ruíz, I., Jiménez, S., Pirone, L., Barrio, R., and Sutherland, J. D. (2011) Generation of stable *Drosophila* cell lines using multicistronic vectors. *Sci. Rep.* **1,** 75 CrossRef Medline
14. Nilsson, T., Hoe, M. H., Slusarewicz, P., Rabouille, C., Watson, R., Hunte, F., Watzele, G., Berger, E. G., and Warren, G. (1994) Kin recognition between medial Golgi enzymes in HeLa cells. *EMBO J.* **13,** 562–574 CrossRef Medline
15. Nilsson, T., Slusarewicz, P., Hoe, M. H., and Warren, G. (1993) Kin recognition: a model for the retention of Golgi enzymes. *FEBS Lett.* **330,** 1–4 CrossRef
16. Yoshida, A., Minowa, M. T., Takamatsu, S., Hara, T., Oguri, S., Ikenaga, H., and Takeuchi, M. (1999) Tissue specific expression and chromosomal mapping of a human UDP-*N*-acetylglucosamine: α1,3-D-mannoside β1,4-*N*-acetylglucosaminyltransferase. *Glycobiology* **9,** 303–310 CrossRef Medline
17. Yoshida, A., Minowa, M. T., Takamatsu, S., Hara, T., Ikenaga, H., and Takeuchi, M. (1998) A novel second isoenzyme of the human UDP-*N*-acetylglucosamine:α1,3-D-mannoside β1,4-*N*-acetylglucosaminyltransferase family: cDNA cloning, expression, and chromosomal assignment. *Glycoconj. J.* **15,** 1115–1123 Medline
18. Kumar, R., Potvin, B., Muller, W. A., and Stanley, P. (1991) Cloning of a human α(1,3)-fucosyltransferase gene that encodes ELFT but does not confer ELAM-1 recognition on Chinese hamster ovary cell transfectants. *J. Biol. Chem.* **266,** 21777–21783 Medline
19. North, S. J., Huang, H. H., Sundaram, S., Jang-Lee, J., Etienne, A. T., Trollope, A., Chalabi, S., Dell, A., Stanley, P., and Haslam, S. M. (2010) Glycomics profiling of Chinese hamster ovary cell glycosylation mutants reveals *N*-glycans of a novel size and complexity. *J. Biol. Chem.* **285,** 5759–5775 CrossRef Medline
20. Bierhuizen, M. F., Hansson, M., Odin, P., Debray, H., Obrink, B., and van Dijk, W. (1989) Structural assessment of the N-linked oligosaccharides of cell-CAM 105 by lectin-agarose affinity chromatography. *Glycoconj. J.* **6,** 195–208 CrossRef Medline
21. Ripka, J., and Stanley, P. (1986) Lectin-resistant CHO cells: selection of four new pea lectin-resistant phenotypes. *Somat. Cell Mol. Genet.* **12,** 51–62 CrossRef Medline
22. Patnaik, S. K., and Stanley, P. (2006) Lectin-resistant CHO glycosylation mutants. *Methods Enzymol.* **416,** 159–182 CrossRef Medline
23. Patnaik, S. K., Zhang, A., Shi, S., and Stanley, P. (2000) α(1,3)Fucosyltransferases expressed by the gain-of-function Chinese hamster ovary glycosylation mutants LEC12, LEC29, and LEC30. *Arch. Biochem. Biophys.* **375,** 322–332 CrossRef Medline
24. Cummings, R. D., Darvill, A. G., Etzler, M. E., and Hahn, M. G. (2015) Glycan-recognizing probes as tools. in *Essentials of Glycobiology* (Varki, A., Cummings, R. D., Esko, J. D., Stanley, P., Hart, G. W., Aebi, M., Darvill, A. G., Kinoshita, T., Packer, N. H., Prestegard, J. H., Schnaar, R. L., and Seeberger, P. H., eds) pp. 611–625, Cold Spring Harbor Laboratory, Cold Spring Harbor, NY
25. Chen, W., and Stanley, P. (2003) Five Lec1 CHO cell mutants have distinct *Mgat1* gene mutations that encode truncated *N*-acetylglucosaminyltransferase I. *Glycobiology* **13,** 43–50 CrossRef Medline
26. Opat, A. S., Houghton, F., and Gleeson, P. A. (2000) Medial Golgi but not late Golgi glycosyltransferases exist as high molecular weight complexes: role of luminal domain in complex formation and localization. *J. Biol. Chem.* **275,** 11836–11845 CrossRef Medline
27. Ioffe, E., and Stanley, P. (1994) Mice lacking *N*-acetylglucosaminyltransferase I activity die at mid-gestation, revealing an essential role for complex or hybrid *N*-linked carbohydrates. *Proc. Natl. Acad. Sci. U.S.A.* **91,** 728–732 CrossRef Medline
28. Metzler, M., Gertz, A., Sarkar, M., Schachter, H., Schrader, J. W., and Marth, J. D. (1994) Complex asparagine-linked oligosaccharides are required for morphogenic events during post-implantation development. *EMBO J.* **13,** 2056–2065 CrossRef Medline
29. Batista, F., Lu, L., Williams, S. A., and Stanley, P. (2012) Complex *N*-glycans are essential, but core 1 and 2 mucin *O*-glycans, *O*-fucose glycans, and NOTCH1 are dispensable, for mammalian spermatogenesis. *Biol. Reprod.* **86,** 179 CrossRef Medline
30. Biswas, B., Batista, F., Sundaram, S., and Stanley, P. (2018) MGAT1 and complex *N*-glycans regulate ERK signaling during spermatogenesis. *Sci. Rep.* **8,** 2022 CrossRef Medline
31. Song, Y., Aglipay, J. A., Bernstein, J. D., Goswami, S., and Stanley, P. (2010) The bisecting GlcNAc on *N*-glycans inhibits growth factor signaling and retards mammary tumor progression. *Cancer Res.* **70,** 3361–3371 CrossRef Medline
32. Zhong, X., Cooley, C., Seth, N., Juo, Z. S., Presman, E., Resendes, N., Kumar, R., Allen, M., Mosyak, L., Stahl, M., Somers, W., and Kriz, R. (2012) Engineering novel Lec1 glycosylation mutants in CHO-DUKX cells: molecular insights and effector modulation of *N*-acetylglucosaminyltransferase I. *Biotechnol. Bioeng.* **109,** 1723–1734 CrossRef Medline
33. Liu, J., Tse, A. G., Chang, H. C., Liu, J., Wang, J., Hussey, R. E., Chishti, Y., Rheinhold, B., Spoerl, R., Nathenson, S. G., Sacchettini, J. C., and Reinherz, E. L. (1996) Crystallization of a deglycosylated T cell receptor (TCR) complexed with an anti-TCR Fab fragment. *J. Biol. Chem.* **271,** 33639–33646 CrossRef Medline
34. Akintayo, A., Liang, M., Bartholdy, B., Batista, F., Aguilan, J., Prendergast, J., Sabrin, A., Sundaram, S., and Stanley, P. (2020) The Golgi glycoprotein MGAT4D is an intrinsic protector of testicular germ cells from mild heat stress. *Sci. Rep.* **10,** 2135 CrossRef Medline
35. Howard, D. R., Fukuda, M., Fukuda, M. N., and Stanley, P. (1987) The GDP-fucose:*N*-acetylglucosaminide 3-α-L-fucosyltransferases of LEC11 and LEC12 Chinese hamster ovary mutants exhibit novel specificities for glycolipid substrates. *J. Biol. Chem.* **262,** 16830–16837 Medline
36. Chaney, W., and Stanley, P. (1986) Lec1A Chinese hamster ovary cell mutants appear to arise from a structural alteration in *N*-acetylglucosaminyltransferase I. *J. Biol. Chem.* **261,** 10551–10557 Medline